Decentralized EV-Based Charging Optimization With Building Integrated Wind Energy

Yu Yang, *Student Member, IEEE*, Qing-Shan Jia, *Senior Member, IEEE*, Xiaohong Guan, *Fellow, IEEE*, Xuan Zhang, Zhifeng Qiu, *Member, IEEE*, and Geert Deconinck, *Senior Member, IEEE*

***Abstract*— Electric vehicles (EVs) have experienced a rapid growth due to the economic and environmental benefits. However, the substantial charging load brings challenging issues to the power grid. Modern technological advances and the huge number of high-rise buildings have promoted the development of distributed energy resources, such as building integrated/mounted wind turbines. The issue to coordinate EV charging with locally generated wind power of buildings can potentially reduce the impacts of EV charging demand on the power grid. As a result, this paper investigates this important problem and three contributions are made. First, the real-time scheduling of EV charging is addressed in a centralized framework based on the ideas of model predictive control, which incorporates the volatile wind power supply of buildings and the random daily driving cycles of EVs among different buildings. Second, an EV-based decentralized charging algorithm (EBDC) is developed to overcome the difficulties due to: 1) the possible lack of global information regarding the charging requirements of all EVs and 2) the computational burden with the increasing number of EVs. Third, we prove that the EBDC method can converge to the optimal solution of the centralized problem over each planning horizon. Moreover, the performance of the EBDC method is assessed through numeric comparisons with an optimal and two heuristic charging strategies (i.e., myopic and greedy). The results demonstrate that the EBDC method can achieve a satisfactory performance in improving the scalability and the balance between the EV charging demand and wind power supply of buildings.**

***Note to Practitioners*—This paper is motivated by the challenging problem due to the substantial charging load of electric vehicles (EVs) on the power grid. Nowadays, modern technological advances and the rapid increase of high-rise buildings have promoted the development of building integrated/mounted wind turbines. As the EVs are usually parked in buildings for a large proportion of time every day, the issue to best utilize locally generated wind power of buildings to suffice EV travelling requirements shows vital significance in reducing their dependence on the power grid. However, there exist two main challenges including: 1) the multiple uncertainties regarding the uncertain wind power generation and the random driving behaviors of EVs and 2) the scalability of the solution method. To tackle the first challenge, the idea of model predictive control is introduced to make charging decisions at each stage based on a short-term prediction of the on-site wind power and the current collection of EVs parked there. To consider the scalability and overcome the lack of global charging information of all EVs in practical deployment, an iterative EV-based decentralized charging algorithm (EBDC) is derived, in which each EV can dynamically update its own charging decisions according to a dynamic charging "price" announced by the buildings. Alternatively, the buildings dynamically adjust the charging "price" to motivate the EVs to get charged during the time periods with sufficient wind power supply. Numeric results demonstrate that the EBDC method is scalable and performs well in improving the balance between the EV charging demand and the wind power supply of buildings.**

***Index Terms*— Building integrated/mounted wind power, decentralized charging algorithm, electric vehicles (EVs), model predictive control (MPC).**

NOMENCLATURE

N	Total number of EVs in the microgrid.
$\mathcal{N}$	Collection of the index for the EVs.
$\mathcal{N}_m(t)$	Collection of EVs parked in building m at time t.
M	Number of buildings in the microgrid.
T_L	Optimization horizon.
T	Planning horizon.
t_0	Beginning of each planning horizon.
Δ_t	Decision interval.
$x_n(t)$	Charging rate of EV n at time t.
$\boldsymbol{x}_n$	Charging profile of EV n over a planning horizon.

Manuscript received May 5, 2018; accepted July 8, 2018. Date of publication September 18, 2018; date of current version July 1, 2019. This work was supported in part by the National Key Research and Development Program of China under Grant 2016YFB0901900 and Grant 2017YFC0704100, in part by the National Natural Science Foundation of China under Grants 61673229, 61174072, 61222302, 91224008, 61221063, 61403429, 61621062, and U1301254, in part by the 111 International Collaboration Project of China under Grant B06002, in part by the Program for New Star of Science and Technology in Beijing under Grant xx2014B056, in part by the Belgium Science Policy Office under Grant FPM2015/ZKD0579, in part by the ISP/13/05TS from the University of Leuven, and in part by the Tsinghua-Berkeley Shenzhen Institute Research Start-Up Funding. This paper was recommended for publication by Associate Editor L. Tang and Editor L. Shi upon evaluation of the reviewers' comments. *(Corresponding author: Qing-Shan Jia.)*

Y. Yang and Q.-S. Jia are with the Center for Intelligent and Networked Systems, Department of Automation, Tsinghua University, Beijing 100084, China (e-mail: yangyu13@mails.tsinghua.edu.cn; jiaqs@tsinghua.edu.cn).

X. Guan is with the Center for Intelligent and Networked Systems, Department of Automation, Tsinghua University, Beijing 100084, China, and also with the Key Laboratory for Intelligent Networks and Network Security Laboratory, Ministry of Education, Xi'an Jiaotong University, Xi'an 710049, China (e-mail: xhguan@tsinghua.edu.cn).

X. Zhang is with the Smart Grid and Renewable Energy Laboratory, Tsinghua–Berkeley Shenzhen Institute, Shenzhen 518055, China.

Z. Qiu is with the Department of Electrical Engineering, Electrical Energy, EnergyVille, Katholieke Universiteit Leuven, 3001 Leuven, Belgium, and also with the Department of Electrical Engineering, Central South University, Changsha 410000, China.

G. Deconinck is with the Department of Electrical Engineering, Electrical Energy, EnergyVille, Katholieke Universiteit Leuven, 3001 Leuven, Belgium.

Color versions of one or more of the figures in this paper are available online at http://ieeexplore.ieee.org.

Digital Object Identifier 10.1109/TASE.2018.2856908

υ_n	Energy consumption rate of EV n (kWh).
$D_n(t)$	Location of EV n at time t.
$B_n(t)$	Stored energy of EV n at time t.
B_n^{cap}	Battery capacity of EV n.
$P_{\max}$	Maximum charging rate for the EVs.
$W_m(t)$	Real wind power of building m at time t.
$\overline{W}_m(t)$	Predicted wind power of building m at time t.
W_m^{cap}	Wind power capacity of building m.
$I_n(t)$	Mobile state of EV n at time t. If $I_n(t)=1$, EV n is mobile at time t, otherwise $I_n(t)=0$.
$t_{n,j}^{\text{dep}}$	Departure time of EV n for its jth parking event.
$L_{n,j}^{\text{Trip}}$	Trip time of EV n for its jth trip event.
$r_n(t)$	Charging "price" for EV n at time t.
$\boldsymbol{r}_n$	Charging "price" profile for EV n over a planning horizon.
$P_m(t)$	Total charging power of EVs in building m at time t.

I. Introduction

OVER the decades, electric vehicles (EVs) have experienced a rapid growth around the world due to technology advances and the urgency for an environmental transportation system. In 2016, the total number of EVs has exceeded one million worldwide, while China accounts for over 30% [1]. The rapid adoption of EVs can potentially achieve environmental advantages. However, the significant EV charging load brings new challenging issues to the reliability of the power grid, such as frequency deviation, voltage rise, higher peak load, and grid congestion [2]–[4].

The exploitation of renewable energy, such as wind power, to charge EVs has been recognized as one promising resolution. Nowadays, it gains extensive popularity to develop distributed energy resources. In particular, technological advances have accelerated the development of building integrated/mounted wind turbines [5]. The challenges of designing wind turbines for buildings to cater urban wind speed, installation space, vibration, and noise restrictions, have been gradually removed [6]. In addition, the number of high-rise buildings has increased rapidly over the years [7]. This reveals great potential to fully explore the wind energy of buildings due to the abundant wind resource and less turbulence [8], [9]. Considering that EVs are usually parked in the parking lots of buildings for more than 90% of the time every day [10], the issue to coordinate EV charging with locally generated wind power of buildings shows various benefits. On the one hand, the variability of wind power can be regulated by scheduling flexible EV charging. On the other hand, the charging demand of EVs can be fully or at least partially supplied by the local renewable generation to help reduce their impacts on the power grid. As a result, this paper investigates the important problem to coordinate EV charging with the locally generated wind power of multiple buildings, which incorporates the random driving requirements of EVs among different buildings. However, there exist several difficulties.

First, there exist multiple uncertainties regarding the volatile wind power supply of buildings and the random charging demand of EVs. *Second*, the problem is a multistage time-correlated decision problem. The daily driving cycle of a vehicle usually consists of multiple consecutive parking or driving events. On the one hand, each individual EV must be charged over a desired level during each parking duration to fulfill its next trip. On the other hand, the charging decisions of a vehicle during the current parking duration will affect its charging decisions afterward. *Third*, the complexity to find an optimal charging strategy for the EVs usually increases rapidly with the number of EVs involved.

Motivated by the challenges mentioned above, the main contributions of this paper are outlined.

1) The real-time coordination of EV charging with the locally generated wind power of multiple buildings is addressed in a centralized framework, which incorporates the volatile wind power of buildings and the random driving requirements of EVs among different types of buildings. Considering the facts that now various forecasting methods can attain a good short-term (minutes to several hours) prediction of wind power output [11], [12] and the charging information (arrival time, departure time, and charging demand) of an EV for each parking duration can be determined upon its arrival at the buildings, the idea of model predictive control (MPC) is introduced to tackle the uncertainties of the problem. The main idea of MPC is to make decision at each stage by solving an optimization problem over a predefined planning horizon but only implement the decisions at the current stage. This process is replicated until the optimization horizon (e.g., one day) is reached [13].
2) An iterative EV-based decentralized charging algorithm (EBDC) is developed to improve scalability. In the decentralized charging algorithm, each individual EV updates its own charging decisions according to the dynamic charging "price" announced by the buildings. Alternatively, the charging "price" is dynamically adjusted by the buildings to motivate the EVs to get charged during the time periods with sufficient local wind power supply.
3) We prove that the EBDC method can converge to an optimal solution of the centralized problem over each planning horizon. Besides, the EBDC method is compared with an optimal and two heuristic charging strategies in several case studies. We conclude that the EBDC method can achieve a satisfactory performance in improving the scalability and the balance between the EV charging demand and the locally generated wind power of buildings.

The remainder of this paper is arranged as follows. In Section II, the related works are discussed. In Section III, the problem to coordinate EV charging with the locally generated wind power of multiple buildings is formulated. In Section VI, the EBDC method is developed. In Section V, numeric comparisons are conducted to evaluate the EBDC method. In Section VI, we briefly conclude this paper.

II. Related Works

Considering the charging flexibility of EVs, many previous studies have endeavored to schedule EV charging with various attempts including charging cost reduction [14], load flattening [15], frequency regulation [16], waiting time minimization [17], and so on. Besides, with the exploitation of distributed renewable energy, the synergy of EV charging with renewable generation begins to attract extensive attention [18].

In terms of the charging control methods for EVs, they are mainly classified as centralized or decentralized. In the centralized control methods, all EVs in the system are usually controlled by a central system operator. For example, Guo *et al.* [19] developed a two-stage framework for the economic operation of an EV parking deck with solar power to maximize its revenue. This method shows good performance, provided that the day-ahead solar output and the EV charging demand can be accurately predicted. Besides, the Markov decision process is acknowledged as another effective approach to tackle the uncertainties associated with the EV charging problem [18], [20]–[24]. This approach can take advantage of the Markov property of the problem; however, it is usually intractable due to the state and the action space explosion. To improve scalability, various electric vehicle aggregators (EVAs) [25]–[28] have been introduced in previous studies. These aggregators are the agents responsible for coordinating the charging demand of a number of vehicles involved. For instance, Mukherjee and Gupta [27] explored the charging scheduling of multiple EVAs to maximize their total profit while maximizing the total number of vehicles charged. The introduction of EVAs can alleviate the complexity due to the increasing number of EVs; however, the performance of the methods greatly depend on how the vehicles are aggregated. Moreover, how to optimally allocate the charging decisions of an EVA to the vehicles involved is still an open question.

Decentralized control methods has been acknowledged as another technique to improve the scalability of the solution methods. In these methods, each individual EV usually determines its own charging profile based on local or global information. However, most of the related works in the literature are heuristic-based [29]. For example, Wu *et al.* [30] established three heuristic dispatching approaches for EVs to improve the match of energy consumption and wind power supply over night. In these heuristic methods, each individual vehicle determines its own charging decisions based on their own charging information and the accumulated load information. Game theory has been acknowledged as another decentralized framework to describe the noncooperative EV charging problem. However, it is usually difficult to find an equilibrium to achieve the optimal performance [15], [31]. For example, Ma *et al.* [15] studied the decentralized charging control of plug-in EVs in a game-theoretic framework with the objective to achieve load "valley." Considering the difficulty to find the equilibrium of the problem, a Nash equilibrium for an infinite population of EVs is derived.

Most of the related works in the literature only consider the charging scheduling of EVs during one parking event or a short time period of the day (e.g., overnight). However, the daily driving cycle of an EV usually consists of multiple consecutive parking and driving events among different locations. The spatial-temporal charging flexibility related to the mobility of EVs [32], [33] has been scarcely addressed in the literature, which is very important to improve the utilization of distributed renewable energy to supply the EV charging demand. Therefore, this paper focuses on the coordination of EV charging with the locally generated wind power of multiple buildings, which incorporates multiple consecutive parking and driving events of each individual EVs among different types buildings (residential, office, and commercial buildings). Moreover, considering that centralized control methods usually encounter various difficulties in practical deployment including: 1) the lack of global information regarding the charging demand of all the EVs; 2) the computation difficulties with the potentially increasing population of EVs; and 3) the reluctancy to abandon the decision-making authority regarding the charging process of their own EVs, this paper is aimed to develop an EBDC for EVs, in which each individual vehicle can determine their own charging decisions based on a dynamically adjusted charging "price."

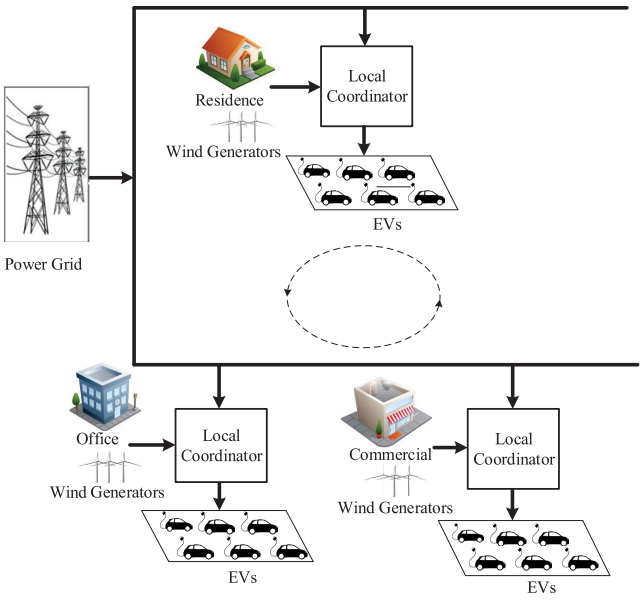

Fig. 1. System architecture.

III. Problem Formulation

In this section, the problem to coordinate EV charging with the locally generated wind power of multiple buildings is formulated with the objective to improve the balance between the EV charging demand and the on-site wind power supply of buildings.

A. System Description

A typical microgrid of buildings [34] is shown in Fig. 1. There exist multiple wind generators-equipped high-rise building and a large number of EVs. The buildings are classified

as residential, office, and commercial buildings (e.g., shopping malls or entertainment centers). The EVs are used to commute between the buildings (e.g., drive to work) or parked in the buildings during their idle time. For example, an office worker may drive to work in the morning from a residential building and park his or her EV in the parking lot of an office building till after work. The daily driving cycles of EVs are random, which usually consists of several consecutive driving and parking events and totally depends on the owners' travel demand. The wind power generated at different buildings is stochastic and weather-dependent. In the microgrid, the locally generated wind power of each building can be used to supply the charging demand of the EVs parked there. When it is not enough to satisfy the charging demand of EVs in time, electricity from the power grid can supplement. The problem is discussed with the objective to best utilize the locally generated wind power of buildings to suffice the EVs' travel requirements, thus reducing their dependence on the power grid. To achieve this, the problem is how to schedule EV charging to coordinate with the uncertain wind power supply of buildings.

In the system, there is a local coordinator corresponding to each building. Besides, an envisioned smart charger, which is capable of decision-making and communication, is assumed to be attached to each vehicle when it arrives at a building. The EV owners are required to report their charging demand (next trip time) and parking duration to the buildings upon arrival. Meanwhile, they can acquire the global information of the environment (e.g., charging "price") through communication with the local coordinators of the buildings.

To achieve the real-time coordination of EV charging demand with local wind power supply of multiple buildings, this paper introduces the idea of MPC concerning the facts that: 1) the wind power output of buildings can be predicted with a high accuracy over a short-term period (minutes to several hours) and 2) the charging demand and remaining parking time of an individual vehicle during a parking duration can be determined upon its arrival at a building. The problem is formulated and solved in a discrete time framework corresponding to $\Delta_t = 30$ minutes' interval with one day equally divided into $T_L = 48$ time slots. The prediction error of the existing wind power forecasting methods for 5 h could be less than 15% [35], [36]; therefore, the planning horizon is selected as $T = 10$ (5 h).

B. System Model

In this section, the problem to schedule EV charging in a microgrid of M buildings is formulated. The charging processes of N EVs indexed by $\mathcal{N} = \{1, 2, \ldots, N\}$ are optimized in a real-time manner to best utilize the locally generated wind power of the buildings to fulfill their travelling requirements. We consider a variable charging rate $x_n(t) \in [0, P_{\max}]$ $(n \in \mathcal{N})$ for the EVs. For notation, $\boldsymbol{x}_n = [x_n(t)](t \in [t_0, t_0 + T])$ denotes the charging profile of EV n over each planning horizon T. Since the EVs may move among or be parked in buildings at different times, we define the location of EV n at time t as $D_n(t) \in \{0, 1, 2, \ldots, M\}$ with the positive integers denoting the buildings and $D_n(t) = 0$ indicating that EV n is mobile at time t.

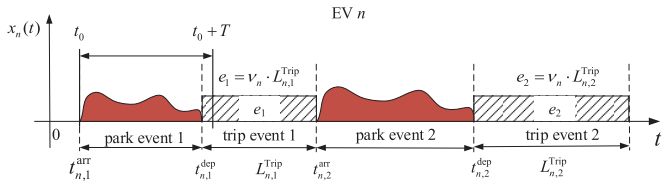

Fig. 2. Charging and energy consumption process of EV n (the energy consumption for the jth trip is computed as $e_j = \nu_n \cdot L^{\text{Trip}}_{n,j}$, $j = 1, 2$).

The dynamics for the stored energy of EV n is described as

$$B_n(t+1) = B_n(t) + x_n(t)\Delta_t - \upsilon_n \Delta_t I_n(t) \quad \forall t = [t_0, t_0 + T]. \tag{1}$$

To ensure the travelling requirements of the owners, the accumulated stored energy of each individual EV should be sufficient to suffice its next trip before its departure time, i.e.,

$$B_n(t_0) + \sum_{t=t_0}^{\min\left(t_0+T, t^{\text{dep}}_{n,j}\right)} x_n(t)\Delta_t + \max\left(t^{\text{dep}}_{n,j} - (t_0 + T), 0\right) P_{\max}\Delta_t \geq \nu_n \cdot L^{\text{Trip}}_{n,j}. \tag{2}$$

Without confusion, we assume that the jth trip event of each vehicle is lagging behind its jth parking event (as Fig. 2). The second term of (2) represents the accumulated charging energy of EV n over the planning horizon, and the third term denotes the maximum possible charging energy of EV n during the remain parking duration. The sum of the two parts should be more than enough to support the EV's next trip.

Meanwhile, the accumulated charging energy of EV n over the planning horizon should not exceed the battery capacity, i.e.,

$$B_n(t_0) + \sum_{t=t_0}^{\min\left(t_0+T, t^{\text{dep}}_{n,j}\right)} x_n(t)\Delta_t \leq B^{\text{cap}}_n. \tag{3}$$

Intuitively, the charging rate of EV n should be constrained by the maximum charging rate of the smart chargers, i.e.,

$$0 \leq x_n(t) \leq P_{\max} \quad \forall t = [t_0, t_0 + T]. \tag{4}$$

Besides, the charging decisions of EV n should be constrained by their arrival and departure times, i.e.,

$$x_n(t) \leq D_n(t) \quad \forall t = [t_0, t_0 + T]. \tag{5}$$

The constraint (5) implies that the EV cannot get charged $(x_n(t) = 0)$ when it is mobile $(D_n(t) = 0)$.

As aforementioned, when the local wind power of buildings is not enough to supply the EV charging demand in time, the procured electricity from the power grid should supplement, which can be calculated as

$$P^c_m(t) = \max(P_m(t) - \overline{W}_m(t), 0) \tag{6}$$

where $P_m(t) = \sum_{n \in \mathcal{N}_m(t_0)} x_n(t)$ is the total charging power of the EVs in building m at time t.

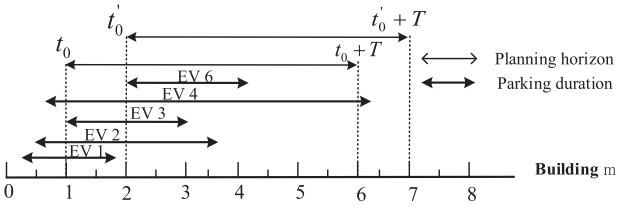

Fig. 3. Current collection of parked vehicles in building m over different planning horizons. $\mathcal{N}_m(t_0) = \{1, 2, 3, 4\}$, $\mathcal{N}_m(t_0') = \{2, 3, 4, 6\}$.

Considering that there may exist load capacity for the building microgrid, we have

$$P_m^c(t) \le \bar{P}^G \quad \forall t \in [t_0, t_0 + T] \tag{7}$$

where $\bar{P}^G$ denotes the maximum amount of power that can be provided to each of the buildings by the power grid.

It is not difficult to note that (6) and (7) can be equivalently described by

$$P_m(t) \le \overline{W}_m(t) + \bar{P}^G \quad \forall t \in [t_0, t_0 + T]. \tag{8}$$

It is acknowledged that the forecasted output of wind power generators can be determined by the forecasted wind speed and turbine parameters. This paper adopts the existing model of [20] to describe the forecasted wind power generation at building m at time t, i.e.,

$$\overline{W}_m(t) = \begin{cases} W_{\text{cap}}^m, & v_{\text{rated}} < v_m(t) \le v_{\text{cutout}} \\ W_{\text{cap}}^m \left(\dfrac{\overline{v}_m(t)}{v_{\text{rated}}}\right)^3, & v_{\text{cutin}} \le \overline{v}_m(t) \le v_{\text{rated}} \\ 0, & \text{otherwise} \end{cases} \tag{9}$$

where $\overline{v}_m(t)$ denotes the forecasted on-site wind speed. v_{cutin}, v_{cutout}, and v_{rated} are the cut-in, cut-out, and rated wind speed for the turbines.

Due to the volatile nature of wind power, it cannot be forecasted with 100% accuracy. To capture the uncertainties of the prediction error, the real wind power output of building m at time t can be assumed as a normal distribution $N(\mu_m(t), (\sigma_m(t))^2)$, with the forecasted wind power $(\mu_m(t))$ as the expected value and a percentage (prediction accuracy) of $\mu_m(t)$ as the prediction error volatility $(\sigma_m(t))$ [37].

As aforementioned, the EV owners are required to report their charging information to the buildings upon arrival. Therefore, the charging information (arrival time, departure time, parking duration, and minimum required charging energy) of the arrived EVs before the beginning of the current planning horizon can be determined. However, the future arrivals are unknown to the buildings unless the random arrival of EVs can be predicted. In this paper, we introduce a sliding window mechanism to incorporate the dynamic arrival and departure of EVs in real-time scheduling. Specifically, at each stage, the charging decisions of the current collection of parked vehicles (having arrived before the beginning of the planning horizon) are considered over the predefined planning horizon. As Fig. 3 shows, at time t_0, the current collection of vehicles parked in building m is described by $\mathcal{N}_m(t_0) \triangleq \{n \in \mathcal{N} | D_n(t_0) = m\}$ (if $n \in \mathcal{N}_m(t_0)$, we have $t_{n,j}^{\text{arr}} \le t_0$). Since in the MPC model only the charging decisions at the current stage (t_0) are implemented, the charging decisions of the arrival EVs during the planning horizon $[t_0, t_0+T]$ will be decided in the following planning horizons. Hereafter, we consider the current collection of parked EVs $(\mathcal{N}_m(t_0), m = 1, 2, \ldots, M)$ over each planning horizon.

The objective of this paper is to best utilize the local wind power supply of the buildings to charge vehicles while satisfying their travel requirements. To achieve this, we define the objective function over each planning horizon as follows:

$$J(t_0; \boldsymbol{x}) = \sum_{t=t_0}^{t_0+T} \sum_{m=1}^{M} [P_m(t) - \overline{W}_m(t)]^2 + \sum_{m=1}^{M} \sum_{n \in \mathcal{N}_m(t_0)} \alpha G_n(t_0 + T) \tag{10}$$

where $\forall t \in [t_0, t_0 + T]$, we define

$$G_n(t) = \frac{v_n \cdot L_{n,j}^{\text{Trip}} - B_n(t_0) - \sum_{t=t_0}^{\min\left(t, t_{n,j}^{\text{dep}}\right)} x_n(t) \Delta_t}{t_{n,j}^{\text{dep}} - t}$$

as the charging incompleteness of EV n at time t. Therefore, $G_n(t_0 + T)$ denotes the charging incompleteness of EV n at the end of the planning horizon $[t_0, t_0 + T]$. The first term of (23) represents the accumulated unbalance between the EV charging demand and the local wind power supply of the buildings. And the second term is used to penalize the unfulfillment of the EV charging demand during the current planning horizon, with α denoting the constant penalty factor. In this case, the EVs will be motivated to charge to the desired levels (satisfying their next trip) as earlier as possible so as to prepare for the new arrival vehicles in the future.

In conclusion, the real-time coordination of EV charging with the local wind power of the buildings can be depicted as

$$\begin{aligned} \min_{\boldsymbol{x}_n, n=1,2,\ldots,N} \quad & J(t_0; \boldsymbol{x}), \quad t_0 = 1, 2, \ldots, T_L \\ \text{Constraints: } & (1)\text{–}(5), \quad n = 1, 2, \ldots, N \\ & (8), \quad m = 1, 2, \ldots, M \end{aligned} \tag{11}$$

where $\boldsymbol{x} = [\boldsymbol{x}_1, \boldsymbol{x}_2, \ldots, \boldsymbol{x}_N]^T$ denotes the collection of the charging profiles of the EVs over the planning horizon.

We note that (11) is a quadratic optimization problem with decoupled constraints [see (1)–(5)] and coupled constraints [see (8)] in terms of the charging decisions for each individual EV. Considering that: 1) the computational burden of the centralized optimization problem increases rapidly with the number of EVs; 2) a centralized approach is not palatable to EV owners, who are accustomed to possess decision-making authority; and 3) it may be difficult to collect the global information concerning the charging requirements of all the EVs due to privacy, an EBDC is necessary and important.

IV. EV-Based Decentralized Charging Algorithm

To eliminate the coupled constraints in (11), we first define the following Lagrangian function, i.e.,

$$\mathrm{L}(t_0; \boldsymbol{x}, \boldsymbol{\lambda}) = J(t_0; \boldsymbol{x}) + \sum_{t=t_0}^{t_0+T} \sum_{m=1}^{M} \lambda_{m,t} \left(P_m(t) - \bar{P}^G - \overline{W}_m(t)\right) \tag{12}$$

where $\boldsymbol{\lambda} = [\lambda_{m,t}] \geq 0$ $(m = 1, 2, \ldots, M, t \in [t_0, t_0 + T])$ are the Lagrangian multipliers.

It is easy to note that when the Lagrangian multipliers are given, the remaining question is how to solve the following optimization problem:

$$\min_{\boldsymbol{x}_n, n=1,2,\ldots,N} \quad \mathtt{L}(t_0; \boldsymbol{x}, \boldsymbol{\lambda})$$
$$\text{Constraints: (1)–(5)}, \quad n = 1, 2, \ldots, N. \tag{13}$$

Since there only exist decoupled constraints in (13), if the local objective function for each EV can be derived, the problem can be decomposed. However, it is easy to note that the global Lagrangian objective function (12) is not decomposable in terms of the EVs. To tackle this difficulty, the main idea of the decentralized charging algorithm in this paper is to design a proper local objective function for each individual EV based on the global Lagrangian objective function in (12).

In this section, we first derive a dynamic charging "price" for each individual EV based on the global Lagrangian objective function (12), i.e.,

$$r_n(t) = \sum_{m=1}^{M} (2(P_m(t) - \overline{W}_m(t)) + \lambda_{m,t}) \delta_{D_n(t_0)=m} - \gamma_n \tag{14}$$

where $\delta_{(\cdot)} \in \{0, 1\}$ is an indicator function, i.e., if EV n is parked in building m at time t_0, we have $\delta_{D_n(t_0)=m} = 1$; otherwise $\delta_{D_n(t_0)=m} = 0$. We define $\gamma_n = \alpha/(t_{n,j}^{\text{dep}} - (t_0 + T))$. Note that the first term of (14) is closely related to the unbalance between the EV charging demand and the local wind power supply of each building. This term is aimed to instruct the vehicles to get charged during the periods with sufficient local wind power supply. Meanwhile, the second term γ_n is related to the charging completeness of EVs, which is aimed to encourage the vehicles to charge as most as possible when there is abundant wind power supply over the current planning horizon.

The charging "price" for EV n can be further derived as follows. We assume the charging decisions for the EVs over the current planning horizon as $\boldsymbol{x} = [\boldsymbol{x}_1, \boldsymbol{x}_2, \ldots, \boldsymbol{x}_N]^T$. Furthermore, we assume that the charging rate of EV n is increased by $\Delta x_n(t)$ at time t (other components of $\boldsymbol{x}$ keep unchanged). In this case, the charging decisions for the EVs are shifted to $\boldsymbol{x}' = \boldsymbol{x} + \Delta x_n(t)$. Here, with a little abuse of notation, we use $\boldsymbol{x} + \Delta x_n(t)$ to represent that the (n, t) element of the matrix $\boldsymbol{x}$ is increased by $\Delta x_n(t)$. As a result, the incremental objective value due to the deviation of the charging decisions for EV n can be calculated as $\mathtt{L}(t_0; \boldsymbol{x} + \Delta x_n(t), \boldsymbol{\lambda}) - \mathtt{L}(t_0; \boldsymbol{x}, \boldsymbol{\lambda}) \approx \sum_{m=1}^{M} \left(2(P_m(t) - \overline{W}_m(t)) + \lambda_{m,t}\right) \delta_{D_n(t_0)=m} \Delta x_n(t) - \gamma_n \Delta x_n(t)$. Thus, the charging "price" for EV n is derived as (14).

With the charging "price" is defined, the total charging "cost" of EV n over the planning horizon can be selected as its local objective function, i.e.,

$$F_n(t_0; \boldsymbol{x}_n) = \sum_{t=t_0}^{t_0+T} r_n(t) x_n(t). \tag{15}$$

Therefore, the subproblem to determine the charging decisions for EV n over the planning horizon can be described as

$$\min_{\boldsymbol{x}_n} \quad F_n(t_0; \boldsymbol{x}_n)$$
$$\text{Constraints: (1)–(5)}. \tag{16}$$

It is easy to note that the above subproblem for EV n will degenerate into a linear programming problem if the charging "price" for EV n ($\boldsymbol{r}_n = [r_n(t)]$, $t \in [t_0, t_0 + T]$) can be determined. However, the charging "prices" for the EVs are unknown before the problem (13) is totally resolved. The charging "price" for each individual EV not only relates to the charging decisions of the other EVs parked in the same buildings, but also depends on its own charging decisions over the planning horizon. To tackle this difficulty, an iterative decentralized charging algorithm is developed to deal with the Lagrangian problem (13).

In the iterative decentralized charging algorithm, the updates for the charging "price" and the charging decisions for the EVs are alternated. Specifically, with a given charging "price," each individual EV acts as an agent and updates their own charging decisions over the planning horizon with the aim to minimize its own charging "cost" defined in (15). Afterward, by collecting the updated charging decisions of the EVs and the predicted wind power output at different buildings, the local coordinator of each buildings will adjust the charging "price" for the vehicles. The two steps mentioned above are alternated until the optimal charging decisions for the EVs are attained. The details of the EBDC to deal with the Lagrangian problem (13) over each planning horizon $[t_0, t_0 + T]$ are described in Algorithm 1.

Algorithm 1 EBDC

1: **Initialization:** $k \leftarrow 0$, $\boldsymbol{x}_n^k = \boldsymbol{0}, \boldsymbol{r}_n^k = \boldsymbol{0}$ $(n \in \mathcal{N}_m(t_0), m = 1, 2, \ldots, M)$, $\boldsymbol{\lambda}^p$.
2: **Iteration:**
3: **for** $n = \mathcal{N}_m(t_0), m = 1, 2, \ldots, M$ **do**
4: Update the charging decisions of EV n, i.e.

$$\boldsymbol{x}_n^{k+1} = \arg\min_{\boldsymbol{x}_n} \sum_{t=t_0}^{t_0+T} \left\{ r_n^k(t) x_n(t) + \beta_{n,t} \left(x_n^k(t) - x_n(t)\right)^2 \right\}$$
$$s.t. \ (1) - (5) \tag{17}$$

5: **end for**
6: **for** $n = \mathcal{N}_m(t_0), m = 1, 2, \ldots, M$ **do**
7: Update the charging "price" $(\forall t \in [t_0, t_0+T])$ for EV n, i.e.

$$P_m^{k+1}(t) = \sum_{n \in \mathcal{N}_m(t_0)} x_n^{k+1}(t)$$
$$r_n^{k+1}(t) = \sum_{m=1}^{M} \left(2(P_m^{k+1}(t) - \overline{W}_m(t)) + \lambda_{m,t}^p\right) \times \delta_{D_n(t_0)=m} - \gamma_n$$

8: **end for**
9: **if** the stopping criterion of (18) is not reached **then** $k \leftarrow k + 1$, go to Step 2.

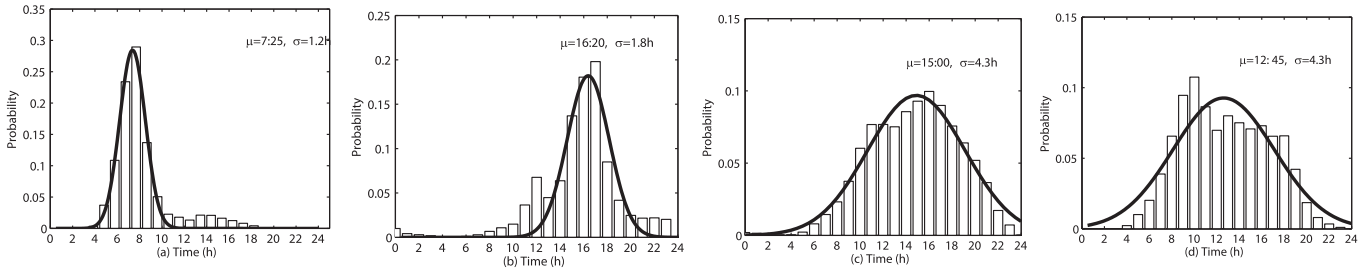

Fig. 4. Distributions of the departure time for EVs from different types of buildings. (a) From residential buildings to office buildings. (b) From office buildings to residential or commercial buildings. (c) From commercial buildings to residential buildings. (d) From residential buildings to commercial buildings.

Algorithm 2 Dual Ascent Algorithm

1: **Initialization:** $p \leftarrow 0$, $\boldsymbol{\lambda}^p = 0$.
2: **Iteration:**
3: **Algorithm** 1
4: $\boldsymbol{x}_n^{p,*} = \boldsymbol{x}_n^k$ $(\forall n \in \mathcal{N})$, $P_m^{p,*}(t) = \sum_{n\in\mathcal{N}_m(t_0)} x_n^{p,*}(t)$ $(m = 1, 2, \ldots, M, \forall t \in [t_0, t_0 + T])$
5: Update the lagrangian multipliers

$$\lambda_{m,t}^{p+1} = [\lambda_{m,t}^p + s^p\big(P_m^{p,*}(t) - \bar{P}^G - \overline{W}_m(t)\big)]_+, \quad m = 1, 2, \ldots, M, \quad \forall t \in [t_0, t_0 + T]$$

6: **if** the stopping criterion of (19) is not reached **then** $k \leftarrow p + 1$, go to Step 2.

In Algorithm 1, the vectors $\boldsymbol{x}_n = [x_n(t)]$ and $\boldsymbol{r}_n = [r_n(t)]$ denote the charging decisions and charging "price" for EV n over the planning horizon. The superscript k represents the number of iterations. The second term of (17) associated with the parameter $\beta_{n,t}$ is a penalty term. This term is added to avoid the oscillation of the iterative decentralized charging algorithm. Specifically, this can be achieved by slowing down the changes of the charging decisions for the vehicles updated at the current iteration (i.e., $\boldsymbol{x}_n^{k+1}$) from the previous iteration ($\boldsymbol{x}_n^k$). Besides, in mathematics, the penalty terms are closely related to the convergence of the iterative decentralized charging algorithm. In the Appendix, we prove that the EBDC method can converge to an optimal solution of problem (13) during each planning horizon, provided that the penalty factors $\beta_{n,t} \geq ((N_m(t_0) + 1)/2)$ if $D_n(t_0) = m$. We note that the subproblem (17) is a quadratic programming problem, which can be easily solved by some existing toolboxes.

To obtain charging decisions for the EVs with a satisfactory performance within an acceptable computing time, the stopping criterion in Algorithm 1 is necessary. In the Appendix, we find that the global Lagrangian objective function (12) will be nonincreasing with the number of iterations over each planning horizon; therefore, we can define the following stopping criterion:

$$|\mathtt{L}(t_0; \boldsymbol{x}^{k+1}, \boldsymbol{\lambda}^p) - \mathtt{L}(t_0; \boldsymbol{x}^k, \boldsymbol{\lambda}^p)|/|\mathtt{L}(t_0; \boldsymbol{x}^k, \boldsymbol{\lambda}^p)| \leq \epsilon_1 \quad (18)$$

where ϵ_1 is a constant threshold.

We should note that Algorithm 1 can be implemented when the Lagrangian multipliers ($\boldsymbol{\lambda}^p$) are given. However, the Lagrangian multipliers relate to the charging decisions of the EVs, which should be dynamically adjusted in the iterative process to ensure that the coupled constraints regarding the load capacity of the building microgrid [see (8)] are satisfied. Therefore, a dual ascent algorithm is developed to update the Lagrangian multipliers as described in Algorithm 2. The subscript p represents the number of iterations for the Lagrangian multipliers. In addition, considering that the dual global objective function will be nondecreasing with the iteration p [38], we define the following stopping criterion for the dual ascent algorithm:

$$|G(t_0; \boldsymbol{x}^{p+1,*}, \boldsymbol{\lambda}^{p+1}) - G(t_0; \boldsymbol{x}^{p,*}, \boldsymbol{\lambda}^p)|/|G(t_0; \boldsymbol{x}^{p,*}, \boldsymbol{\lambda}^p)| \leq \epsilon_2 \quad (19)$$

where we have the global Lagrangian dual function $G(t_0; \boldsymbol{x}^{p,*}, \boldsymbol{\lambda}^p) = \mathtt{L}(t_0; \boldsymbol{x}^{p,*}, \boldsymbol{\lambda}^p)$. ϵ_2 is a constant threshold.

V. Numeric Results

In this section, we first analyze the temporal and spatial stochastic characteristics of the EVs' driving and parking behaviors based on real-world travel data. Afterward, several numeric experiments are conducted to evaluate the performance and scalability of the decentralized charging algorithm proposed in this paper.

A. Statistical Driving and Parking Behaviors of EVs

In the literature, a few works have investigated the random driving and parking behaviors of EVs from different perspectives [39], [40]. However, the spatial stochastic characteristics of EV driving and parking have been less discussed, which are important concerning the EV scheduling in smart distribution grids. In this section, the temporal and spatial stochastic characteristics of EV driving and parking among different types of buildings (residential, office and commercial buildings) are explored based on the real data from the 2009 National Household Travel Survey (NHTS) [41].

As aforementioned, the daily driving cycles of EVs usually consist of several individual trips among different buildings. To explore the temporal and spatial stochastic characteristics of EV driving the behaviors of EVs among different types of buildings, the trips from NHTS are mainly classified as "residential-to-office," "office-to-residential," "office-to-commercial," and "residential-to-commercial" (other kinds of trips are ignored). Based on the acquired data, the departure time distributions of vehicles from one building to another are plotted in histograms as Fig. 4. This implies that the distributions of the EV departure time from different types

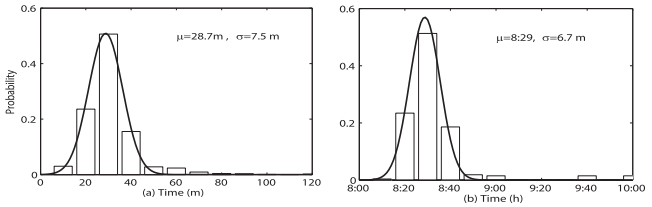

Fig. 5. Distributions of the trip time and arrival time of the vehicles' departure from a residential building to an office building at 8:00.

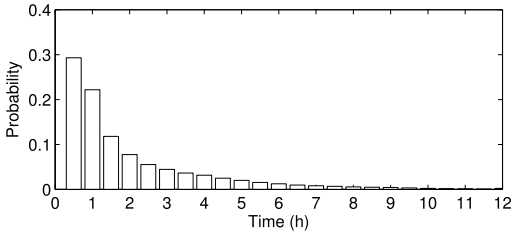

Fig. 6. Distribution of the parking time in commercial buildings.

of buildings can be approximated by Gaussian distributions with different parameters. For example, the departure time of EVs from residential buildings to office buildings shows Gaussian-like distribution with mean 7:25 and a standard deviation of 1.2 h. Moreover, we find that the departure time windows of the vehicles from the residential and office buildings correspond well to the general commuting time of work with a small deviation. However, the departure time of vehicles commuting between residential and commercial buildings demonstrates a relatively larger volatility.

Intuitively, the arrival time of vehicles at a building is determined by the departure time from the previous location and the trip time between them. To illustrate it, we investigate the relationship between the arrival time and the trip time of the EVs that depart from a residential building at 8:00 to an office building with a 30-km distance. The arrival time and the trip time for those vehicles are plotted in histogram as Fig. 5(a) and (b). We find that the arrival time of those vehicles shows a similar Gaussian distribution compared with the vehicles' trip time. Therefore, the distribution of EVs' arrival time at a building can be derived from the departure time from a starting building and the stochastic trip time between them, i.e.,

$$P^{m,j}_{\mathrm{ARR}}(t_{\mathrm{arr}}) = \int_{t_{\mathrm{dep}}<t_{\mathrm{arr}}} P^{m,j}_{\mathrm{TRIP,DEP}}(t_{\mathrm{trip}} = t_{\mathrm{arr}} - t_{\mathrm{dep}}|t_{\mathrm{dep}}) \times P^{m,j}_{\mathrm{DEP}}(t_{\mathrm{dep}})dt_{\mathrm{dep}} \quad (20)$$

where $P^{m,j}_{\mathrm{ARR}}(t_{\mathrm{arr}})$ is the probability density function (pdf) of the EVs' arrival time from building m to building j. $P^{m,j}_{\mathrm{TRIP,DEP}}(t_{\mathrm{trip}}|t_{\mathrm{dep}})$ is the conditional pdf of the trip time for vehicles' departure from building m at time t_{dep} to building j. $P^{m,j}_{\mathrm{DEP}}(t_{\mathrm{dep}})$ is the pdf of the departure time from building m to building j.

As aforementioned, the departure time of vehicles from commercial buildings demonstrates a relatively larger volatility. Therefore, the probability of EVs' different parking durations in commercial buildings is analyzed based on the acquired data, which are plotted in histograms as Fig. 6.

B. Parameters' Setting

A microgrid composed of $M = 5$ high-rise buildings (two residential buildings, two office buildings, and one shopping mall) is considered. The maximum charging power of EVs is set as $P_{\max} = 6$ kW, which refers to the state grid EV charging standards [42]. The energy consumption rate $\nu_n = 5$ kWh for the EVs is derived from the average driving speed of passenger cars in Beijing (20–40 km/h) [43] and the electric energy efficiency of BYD e6 (0.2 kWh/km). The penalty factors for the charging incompleteness of the EVs over each planning horizon are set as $\alpha = 5$. The major usage of EVs consists of commuting between home and workplace and travelling for shopping or entertainment. In Section V-A, we derive that the departure time of EVs from residential buildings to office buildings can be described as a normal distribution $N(7{:}25, (1.2\ \mathrm{h})^2)$. And the departure time of vehicles from office buildings to residential or commercial buildings obeys a normal distribution $N(16{:}20, (1.8\ \mathrm{h})^2)$. The departure time from commercial buildings to residential buildings can be described by normal distribution $N(15{:}00, (4.3\ \mathrm{h})^2)$. And the departure time from residential buildings to commercial buildings can be described as $N(12{:}45, (4.3\ \mathrm{h})^2)$. Besides, we derive from the acquired data that the vehicles are driven to work (an office building) in the morning with a probability of $p_1 = 0.72$ or to a shopping center (a commercial building) with a probability of $(1 - p_1) = 0.28$. And an EV user will drive to home after work with a probability of $p_2 = 0.78$ or to a shopping center with a probability of $(1 - p_2) = 0.22$.

The trip time of EVs depends on the distance between two buildings, vehicle velocity, and road congestion. To capture the uncertainties, normal distributions with different parameters are used to describe the variations in the trip time between different buildings. They are listed in Table II. For instance, the trip time of EVs between residential building I and office building I obeys a normal distribution $N(1.0\ \mathrm{h}, (0.5\ \mathrm{h})^2)$.

Considering that the EV users may live or work in different places, we use Table II to denote the percentage of people living or working in the two residential or office buildings. For instance, 40% of the EV users live in Residential I, among which 70% work in Office I and the remaining 30% work in Office II.

The parameters of wind turbines ($\upsilon_{\mathrm{cutin}} = 3.5$ m/s, $\upsilon_{\mathrm{cutout}} = 25$ m/s, and $\upsilon_{\mathrm{rated}} = 10$ m/s) are set based on most commercial wind turbines. The Rayleigh model ($\overline{u}$) is adopted to describe the variations in wind speed at the buildings [44]. The average wind speed $\overline{u} = 3.6$ m/s is derived from the observations at the Beijing Capital Airport from June 2009 to March 2016 [45]. In the decentralized charging algorithm, the penalty factors are set as $\beta_{n,t} = \lceil((N_m(t_0) + 1)/2)\rceil$ if $D_n(t_0) = m$ $(n \in \mathcal{N})$.

C. Performance Evaluation

In this section, we consider two case studies with $N = 50$ and $N = 100$ EVs to evaluate the performance of the EBDC method in improving the balance between the EV charging

TABLE I
DISTRIBUTION OF TRIP TIME BETWEEN $M = 5$ BUILDINGS

	Office I	Office II	Commercial
Residential I	$N(1.0, (0.5)^2)$	$N(1.5, (0.5)^2)$	$N(1.0, (0.5)^2)$
Residential II	$N(0.5, (0.5)^2)$	$N(1.5, (0.5)^2)$	$N(1.5, (0.5)^2)$
Commercial	$N(1.0, (0.5)^2)$	$N(1.0, (0.5)^2)$	-

TABLE II
DISTRIBUTION OF EV USERS IN THE RESIDENTIAL AND OFFICE BUILDINGS

Residence	Percentage	Working Place	Percentage
Residential I	40%	Office I	70%
		Office II	30%
Residential II	60%	Office I	40%
		Office II	60%

demand and the local wind power supply of the buildings. The charging strategy obtained from the EBDC method is compared with the optimal charging strategy (Opt), myopic charging strategy (MYO), and a greedy charging strategy (Greedy).

1) *Opt:* The optimal solution to maximize the balance between the EV charging demand and the local wind power supply of buildings depends on the global information including: a) the daily driving cycles of EVs among the buildings and b) the day-ahead accurate prediction of the wind power supply at each buildings. However, they are usually difficult to acquire in practical deployment. In the comparative studies, we assume that the global information is known in scheduling; therefore, the optimal charging strategy can be attained by solving a deterministic quadratic optimization problem, i.e.,

$$\min \sum_{t=1}^{T_L} \sum_{m=1}^{M} \left(P_m^{\mathrm{EV}}(t) - W_m(t)\right)^2$$

$$\text{s.t. } B_n\left(t_{n,j}^{\mathrm{arr}}\right) + \sum_{t=t_{n,j}^{\mathrm{arr}}}^{t_{n,j}^{\mathrm{dep}}} x_n(t)\Delta_t \geq L_{n,j}^{\mathrm{trip}} \cdot \nu_n \tag{21a}$$

$$B_n\left(t_{n,j}^{\mathrm{arr}}\right) + \sum_{t=t_{n,j}^{\mathrm{arr}}}^{t_{n,j}^{\mathrm{dep}}} x_n(t)\Delta_t \leq B_n^{\mathrm{cap}} \tag{21b}$$

$$\forall j = 1, 2, \ldots, N_n^{\mathrm{Trip}} \tag{21c}$$

$$B_n(t+1) = B_n(t) + x_n(t)\Delta_t - \nu_n I_n(t) \tag{21d}$$

$$0 \leq x_n(t) \leq P_{\max} \tag{21e}$$

$$x_n(t) \leq D_n(t) \quad \forall t = 1, 2, \ldots, T_L \tag{21f}$$

$$P_m^{\mathrm{EV}}(t) \leq \overline{W}_m(t) + \bar{P}^G$$
$$m = 1, 2, \ldots, M \quad \forall t = 1, 2, \ldots, T_L \tag{21g}$$

where $P_m^{\mathrm{EV}}(t) = \sum_{\mathcal{N}_m(t)} x_n(t)$ represents the total charging power of the EVs in building m at time t. N_n^{trip} is the total number of daily trips of EV n.

2) *MYO:* At each stage, the number of EVs to get charged with a maximum charging rate ($P_{\max}$) is determined based on the predicted wind power output at each building. However, the charging demand of the EVs should be sufficed in time to guarantee their travelling requirements.

3) *Greedy:* During each parking duration, each EV begins to get charged with a maximum charging rate ($P_{\max}$) upon arrival at the buildings until the required charging energy is reached.

We define the basic wind power capacity for $M = 5$ buildings (Residential I, Residential II, Office I, Office II, and Commercial) as $W_{\mathrm{cap}} = [20\ 20\ 28\ 30\ 15]$ (kW). In the two case studies, the wind power capacity for the buildings is set as W_{cap} ($N = 50$) and $2W_{\mathrm{cap}}$ ($N = 100$), respectively. Considering that there exists randomness both in the locally generated wind power of buildings and the dynamic arrival and departure of vehicles, $S = 50$ sample paths concerning the wind power of buildings and the daily driving cycles of EVs are generated based on the derived probability distributions. In particular, the sample paths for the predicted wind power are generated based on the real wind power generations of each building with 20% prediction error.

In order to guarantee the travelling requirements of the owners, the EVs must be charged to their desired level before the departure time. Therefore, there exist minimum load capacity for the buildings $\bar{P}_{\min}^G$, which can be determined by solving the following problem:

$$\min \ \bar{P}^G$$
$$\text{Constraints: (21a)–(21f).} \tag{22}$$

In the two case studies ($N = 50$ and $N = 100$), the charging strategies obtained from the EBDC method with or without load capacity constraints are studied. When there is no load capacity limits ($\bar{P}^G$ is large enough), the charging strategy can be derived based on Algorithm 1 with $\boldsymbol{\lambda}^p = \mathbf{0}$. Besides, in the case studies with load capacity constraints, we set $\bar{P}^G = 1.2\bar{P}_{\min}^G$ kW. The step size of the dual ascent algorithm is set as $s^p = 0.8$.

In the two case studies, the distributions of the unbalance between the EV charging demand and the local wind power supply of the buildings under different charging strategies are plotted in histograms as Fig. 7 ($N = 50$) and Fig. 8 ($N = 100$). We see that the average unbalance between the EV charging demand and the local wind power supply of buildings using the myopic charging strategy is apparently reduced compared with the greedy charging strategy. The result is attributed to that the one-step prediction information about the wind power generation of buildings is incorporated in the myopic charging strategy. We first analyze the performance of the EBDC method when there is no load capacity (or load capacity is large enough) in the building microgrid. We find that the unbalance between the EV charging demand and wind power supply of buildings using the EBDC method has been reduced by 68.4% ($N = 50$) and 61.1% ($N = 100$) compared with the greedy charging strategy. Moreover, form Fig. 7(a) and (b), we see that the EBDC method can achieve a close performance compared with the optimal charging strategy in improving the balance between the EV charging demand and the local wind power supply of multiple buildings. The minor differences

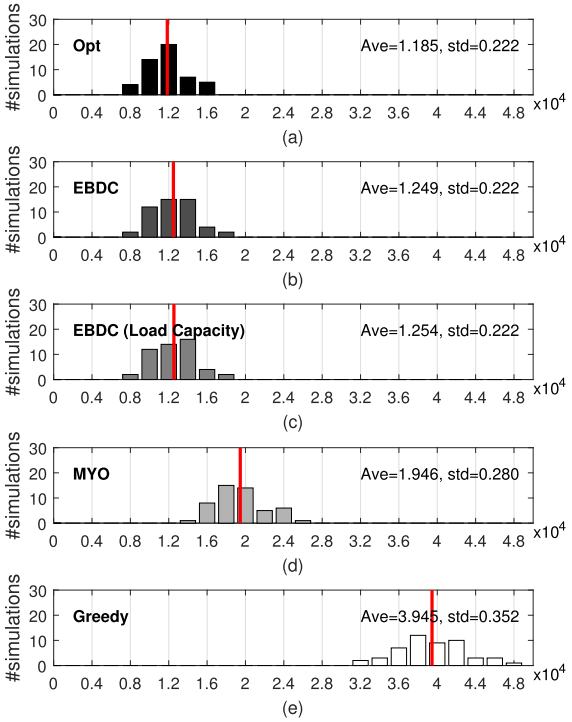

Fig. 7. Unbalance between the EV charging demand of $N = 50$ EVs and the local wind power supply of the buildings. (a) Optimal. (b) EBDC (without load capacity constraints). (c) EBDC. (d) Myopic. (e) Greedy.

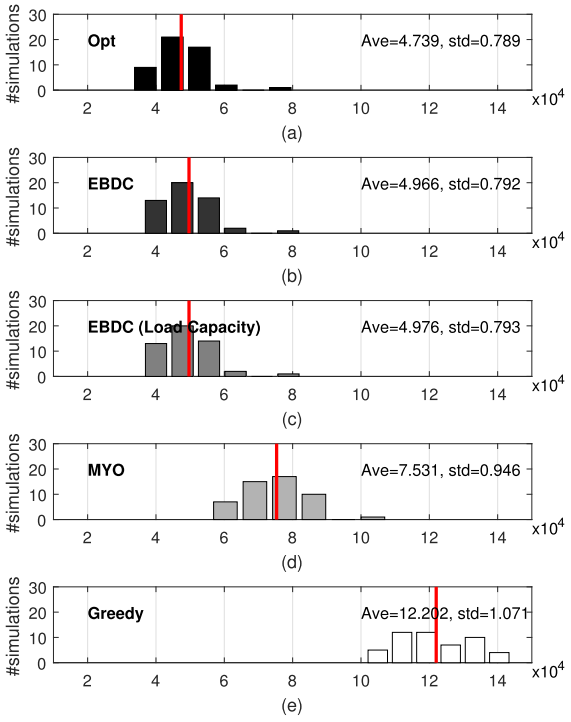

Fig. 8. Unbalance between the EV charging demand of $N = 100$ EVs and the local wind power supply of the buildings. (a) Optimal. (b) EBDC. (c) EBDC (with load capacity constraints). (d) Myopic. (e) Greedy.

5.9% ($N = 50$) and 4.9% ($N = 100$) of the EBDC method compared with the optimal charging strategy are caused by the incomplete information about the EV charging requirements and the prediction error on the wind power output of buildings in real-time scheduling. Moreover, we find that the standard deviation (std.) of the unbalance using the EBDC is almost the same compared with the optimal charging strategy. This implies that the EBDC method performs well in incorporating the dynamic arrival and departure of the EVs in the scheduling.

Besides, from Fig. 7(b) and (c) [Fig. 8(b) and (c)], we note that there exist a minor difference (gap) between the performance of the charging strategies obtained from the EBDC method with and without load capacity constraints. When the load capacity is set as $\bar{P}^G = 1.2\bar{P}^G_{\min}$ kW, the accumulated unbalance between the on-site wind power generation and the EV charging demand has been increased by 0.4% ($N = 50$) and 0.2% ($N = 100$). The phenomenon are reasonable, because some new constraints are added in the optimization problem.

D. Complexity and Scalability

In practical deployment, the EV owners are usually willing to participate in the scheduling provided that their travelling requirements are guaranteed. It is not difficult to interpret that when the load capacity $\bar{P}^G$ is large enough, the travelling requirements of all EVs can be guaranteed, otherwise may not. Therefore, in the subsequent numerical experiments of this section, we assume that the load capacity of the building microgrid is large enough to supply the surplus charging demand of EVs. In this regard, the decentralized charging strategy for the EVs can be obtained based on Algorithm 1 with $\boldsymbol{\lambda}^p = \mathbf{0}$.

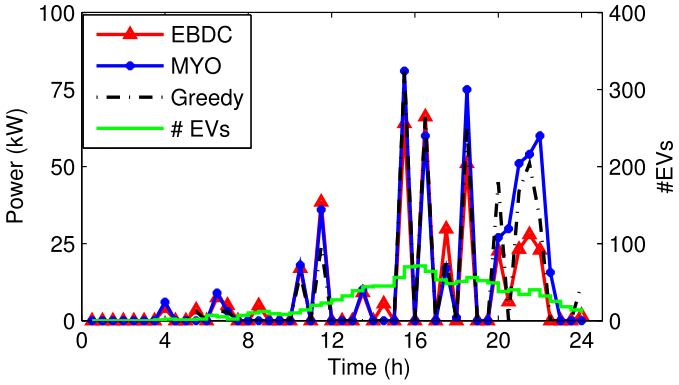

Fig. 9. Amount of power from the power grid at the commercial building ($N = 1000$).

In this section, a number of case studies with a larger population of EVs, i.e., $N = 200$, $N = 300$, $N = 500$, $N = 800$, and $N = 1000$, are conducted to evaluate the complexity and scalability of the EBDC method. The wind power capacity for the buildings is set as 2 W_{cap} ($N = 100$), 3 W_{cap} ($N = 200$), 4.5 W_{cap} ($N = 300$), 8 W_{cap} ($N = 500$), 9 W_{cap} ($N = 800$), and 12 W_{cap} ($N = 1000$). The stopping criterion is set as $\epsilon_1 = 0.02$. Since each individual EV only needs to update its own charging decisions by solving a small subproblem at each iteration, the EBDC method is scalable. Considering that it will be time-consuming to solve the centralized optimization problem (21), even if the global

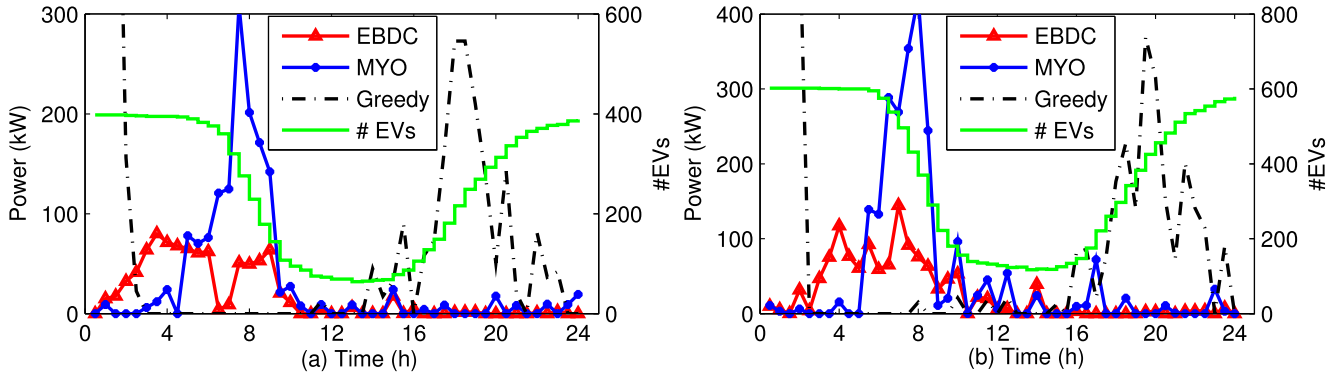

Fig. 10. Amount of power from the power grid at the residential buildings ($N = 1000$). (a) Residential I. (b) Residential II.

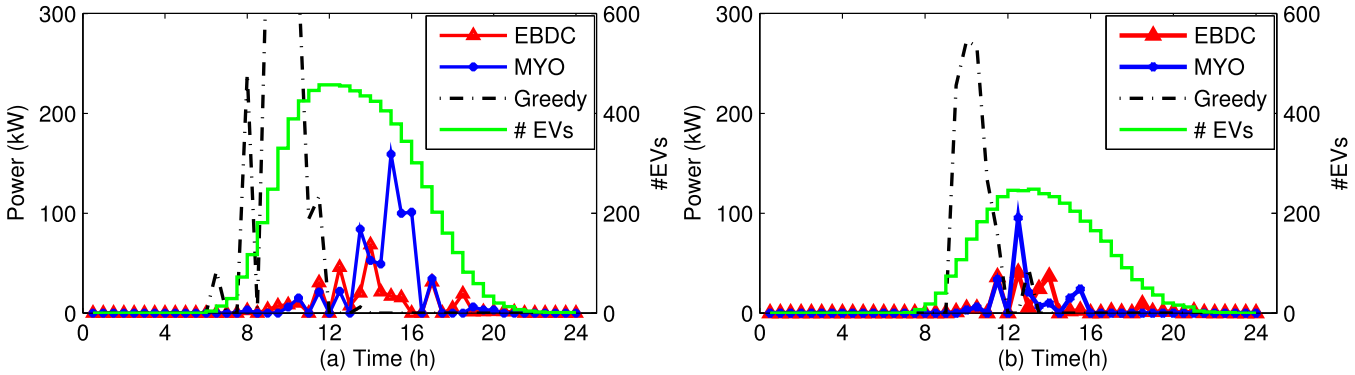

Fig. 11. Amount of power from the power grid at the office buildings ($N = 1000$). (a) Office I. (b) Office II.

TABLE III
UNBALANCE BETWEEN THE EV CHARGING DEMAND AND THE ON-SITE WIND POWER SUPPLY OF THE BUILDINGS

	Greedy $\times 10^4$		MYO $\times 10^4$		EBDC $\times 10^4$	
	mean	std.	mean	std.	mean	std.
$N = 100$	12.20	1.07	7.53	0.95	4.74	0.79
$N = 200$	58.19	4.11	17.26	2.58	10.81	1.77
$N = 300$	130.06	7.54	37.64	4.76	24.06	3.61
$N = 500$	382.96	23.31	122.14	18.26	79.82	13.50
$N = 800$	823.21	45.88	180.22	21.30	112.39	17.28
$N = 1000$	1308.23	73.85	293.13	34.33	187.08	25.69

information regarding the day-ahead wind power generation of the buildings and the daily driving cycles of EVs can be acquired, the EBDC is compared with the two heuristic charging strategies (myopic and greedy) in this section.

Similarly, $S = 50$ sample paths are generated in each case study to evaluate the performance of different charging strategies. The mean and standard deviation (std.) of the unbalance between the EV charging demand and local wind power supply of the buildings are listed in Table III. We conclude that both the mean and standard deviation of the unbalance between the supply and demand are apparently reduced using the EBDC method compared with the two charging strategies. Specifically, the decentralized charging strategies obtained from the EBDC method outperform the greedy and the myopic charging strategy with about 60%–80% and 34%–37% less unbalance, which are consistent with the numeric results in Section V-B. This implies that the EBDC method can still achieve a satisfactory performance when applied to larger scale problems.

Besides, to evaluate the charging strategies in reducing the dependence of the EV charging demand on the power grid, the procured electricity of different buildings ($P_m^c(t)$) from the power grid is studied. We consider a special case (a sample path) with $N = 1000$ EVs in the microgrid; the curves of the procured electricity of different buildings under different charging strategies are displayed in Fig. 9 (commercial), Fig. 10 (residential), and Fig. 11 (office). We see that the EBDC can apparently reduce the amount of the procured power by the buildings from the power grid to satisfy the surplus charging demand of the EVs compared with the two heuristic charging strategies. This implies that the EBDC method can effectively improve the utilization of wind power while supplying the charging demand of the EVs. Moreover, we may observe some phenomenon that coincides with the general driving behaviors of the EV owners. Specifically, we see that the charging peaks of the residential buildings appear from the late evening to the morning. This is attributed to the fact that a large number of vehicles are driven back to the residential area and needed to get charged. Besides, we observe that a massive number of vehicles need to get charged between 9:00 and 18:00 in the office buildings. This time period corresponds well to the general working hours. Different from the residential and office buildings, a high charging peak appears in the commercial building

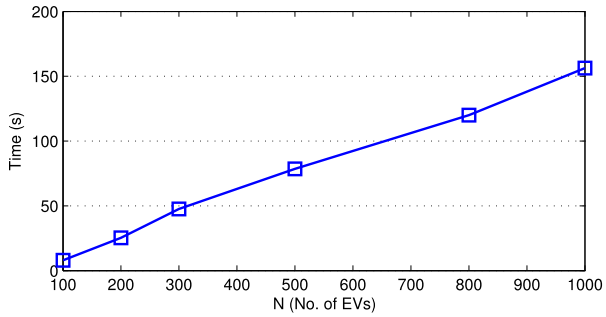

Fig. 12. Average computing time at each stage with the number of EVs.

during 12:00–21:00. This phenomenon is due to the fact that people tend to go shopping or have recreations in the afternoon and in the evening.

To further investigate the scalability of the EBDC method, the average computing time at each stage is studied. The subproblems are solved using MATLAB (R2016a) on Windows 7 with a main frequency of 3.2 GHz. The average computing time at each stage with different number of EVs is shown in Fig. 12. We observe that the average computing time at each stage approximately increases linearly with the number of EVs. This is reasonable because the main computation of the EBDC method is for each individual EV to iteratively update their own charging decisions at each stage. Besides, we note that the average computing time at each stage is about 2.5 min $\ll \Delta_t$ for $N = 1000$ EVs. This implies that the EBDC is time-efficient in real-time scheduling. Moreover, we may note from Algorithm 1 that at each iteration, the EV agents can update their charging decisions in parallel; therefore, in practical deployment, the computation efficiency of the EBDC method can be further improved.

VI. Discussion

Considering that future buildings may be integrated with various renewable energy, this section briefly discusses the case where each building is integrated with wind generators and PV arrays. In this case, to best utilize the local renewable generation to supply the EV charging demand, the global objective function in (23) can be modified to

$$J(t_0; \boldsymbol{x}) = \sum_{t=t_0}^{t_0+T} \sum_{m=1}^{M} [P_m(t) - \overline{W}_m(t) - \overline{V}_m(t)]^2 + \sum_{m=1}^{M} \sum_{n \in \mathcal{N}_m(t_0)} \alpha G_n(t_0 + T) \quad (23)$$

where $\overline{V}_m(t)$ denotes the predicted solar generation of building m at time t.

Accordingly, in the EBDC method, the charging "price" in (14) should be replaced by

$$r_n(t) = \sum_{m=1}^{M} 2(P_m(t) - \overline{W}_m(t) - \overline{V}_m(t))\delta_{D_n(t_0)=m} - \gamma_n. \quad (24)$$

Similarly, the decentralized charging strategy for the EVs can be obtained based on Algorithm 1.

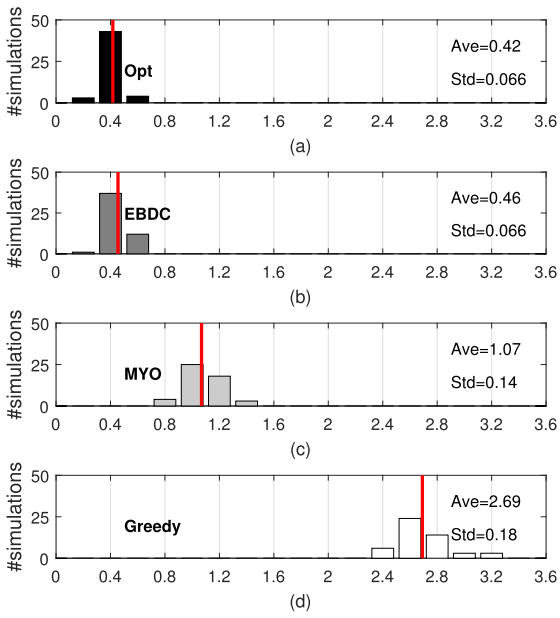

Fig. 13. Unbalance between the EV charging demand of $N = 50$ EVs and the local renewable energy supply of the buildings. (a) Optimal. (b) EBDC. (c) Myopic. (d) Greedy.

To evaluate the performance of the EBDC method applied to the case with multiple distributed renewable generation (i.e., wind and solar power) in the microgrid, we conduct a case study with $N = 50$ EVs. The rated wind and solar power capacity for the buildings are set as $W_{\text{cap}} = [10\ 10\ 15\ 15\ 10]$ kW and $V_{\text{cap}} = [10\ 10\ 15\ 15\ 10]$ kW, respectively. The models regarding solar generation refer to [46]–[48]. The other parameters are the same as described in Section V-B.

Accordingly, to obtain the optimal charging strategy for the EVs to maximize the balance between the EV charging demand and the local renewable energy supply, the global objective function in (21) should be replaced by

$$\min \sum_{t=1}^{T_L} \sum_{m=1}^{M} \left(P_m^{\text{EV}}(t) - W_m(t) - V_m(t)\right)^2. \quad (25)$$

In the case study, the decentralized charging strategy of the EBDC method is compared with the optimal charging strategy and the two heuristic charging strategies (myopic and greedy). Similarly, $S = 50$ sample paths are generated to assess the performance of different charging strategies. The distribution of the unbalance between the EV charging demand and the local renewable energy supply of the buildings under different charging strategies is plotted in histograms as Fig. 13. From the case study, we note that the EBDC method can still achieve a close performance compared with the optimal charging strategy in improving the balance between the supply and demand in the building microgrid. The minor difference of the objective value (9.8%) under the optimal charging strategy and the charging strategy from the EBDC method is attributed to the prediction error of the on-site renewable generation (wind power and solar power) of buildings.

VII. Conclusion

This paper investigates the coordination of EV charging with the locally generated wind power of multiple buildings. The problem is formulated in a centralized framework with the objective to improve the balance between the EV charging demand and the local wind power supply of buildings. To tackle the uncertainties, the idea of MPC is introduced, which makes decision at each stage based on the predicted wind power output of the buildings and the current collection of parked EVs over a predefined planning horizon. By exploring the structure of the centralized problem, an EBDC is developed, in which each individual EV agent can dynamically update their own charging decision based on the charging "price" announced by the buildings. We prove that the EBDC method can converge to an optimal solution of the centralized problem. Moreover, the performance of the EBDC is assessed through comparisons with an optimal and two heuristic charging strategies (i.e., greedy and myopic). We conclude that the EBDC method is scalable and performs well in improving the balance between the EV charging demand and the local wind power supply. Furthermore, the extension of the decentralized method is discussed and preliminarily conclude that the current method still applies to the case where there exist multiple renewable generation, such as building integrated wind power and PVs. Note that it is an interesting future work to coordinate the charging of EVs with the multienergy systems in smart buildings [48]–[54], both of which are flexible loads. Then, one may need to combine the methods in this paper with event-based optimization [55] to address the even larger optimization problem.

Appendix
Proof of the Convergence of the EV-Based Decentralized Method

In this section, we endeavor to prove that the EBDC can converge to an optimal solution of the centralized Lagrangian problem in (13) over each planning horizon $[t_0, t_0 + T]$.

In Algorithm 1, we note that the subproblem associated with EV n at iteration $k+1$ is a convex optimization problem with the charging "price" $\boldsymbol{r}_n^k = [r_n^k(t)]$ given. Thus, we can derive from the first order optimality condition that

$$\sum_{t=t_0}^{t_0+T} \left[r_n^k(t) + 2\beta_{n,t}\left(x_n^{k+1}(t) - x_n^k(t)\right)\right]\left(x_n(t) - x_n^{k+1}(t)\right) \geq 0 \quad \forall \boldsymbol{x}_n \in \mathcal{X}_n \tag{26}$$

where we should note that the obtained charging decision $\boldsymbol{x}_n^{k+1} = [x_n^{k+1}(t)]$ at iteration $k+1$ is the optimal solution of problem (17). $\mathcal{X}_n$ denotes the feasible charging decisions for EV n over the planning horizon, which is a convex set composed by (1)–(5).

It is straightforward that $\boldsymbol{x}_n^k$ is a feasible charging decision for EV n over the planning horizon $[t_0, t_0 + T]$; thus, we have

$$\sum_{t=t_0}^{t_0+T} r_n^k(t)\left(x_n^{k+1}(t) - x_n^k(t)\right) \leq -\sum_{t=t_0}^{t_0+T} 2\beta_{n,t}\left(x_n^{k+1}(t) - x_n^k(t)\right)^2 \tag{27}$$

where $r_n^k(t) = \sum_{m=1}^{M} 2(P_m^k(t) - \overline{W}_m(t) + \lambda_{m,t}^p)\delta_{D_n(t_0)=m} - \gamma_n$ as defined in (14).

We summarize (27) for all $n \in \mathcal{N}_m(t_0)$; thus, we have

$$\begin{aligned}
&\sum_{t=t_0}^{t_0+T} \left(2\left(P_m^k(t) - \overline{W}_m(t)\right) + \lambda_{m,t}^p\right)\left(P_m^{k+1}(t) - P_m^k(t)\right) \\
&\leq \sum_{t=t_0}^{t_0+T} \sum_{n=\mathcal{N}_m(t_0)} \Big[\gamma_n\left(x_n^{k+1}(t) - x_n^k(t)\right) \\
&\qquad - 2\beta_{n,t}\left(x_n^{k+1}(t) - x_n^k(t)\right)^2\Big]
\end{aligned} \tag{28}$$

where $P_m^k(t) = \sum_{n\in\mathcal{N}_m(t_0)} x_n^k(t)$.

As defined, the global Lagrangian objective function at iteration k can be described as

$$\begin{aligned}
&\mathrm{L}(t_0; \boldsymbol{x}^k, \boldsymbol{\lambda}^p) \\
&= \sum_{t=t_0}^{t_0+T} \sum_{m=1}^{M} \left[P_m^k(t) - \overline{W}_m(t)\right]^2 \\
&\quad + \sum_{n=1}^{N} \gamma_n \left(\nu_n \cdot L_{n,j}^{\mathrm{Trip}} - B_n(t_0) - \sum_{t=t_0}^{\min\left(t_0+T, t_{n,j}^{\mathrm{dep}}\right)} x_n(t)\Delta_t\right) \\
&\quad + \sum_{m=1}^{M} \lambda_{m,t}\left(P_m(t) - \bar{P}^G - \overline{W}_m(t)\right)
\end{aligned} \tag{29}$$

where we have $\boldsymbol{x}^k = [\boldsymbol{x}_n^k, \ldots, \boldsymbol{x}_N^k]$, with $\boldsymbol{x}_n^k$ denoting the charging profile of EV n over the planning horizon obtained at iteration k.

The difference in the global Lagrangian objective function at two successive iterations can be computed as

$$\begin{aligned}
&\mathrm{L}(t_0; \boldsymbol{x}^{k+1}, \boldsymbol{\lambda}^p) - \mathrm{L}(t_0; \boldsymbol{x}^k, \boldsymbol{\lambda}^p) \\
&= \sum_{t=t_0}^{t_0+T} \sum_{m=1}^{M} 2\left[P_m^{k+1}(t) - P_m^k(t)\right]\left[P_m^k(t) - \overline{W}_m(t)\right] \\
&\quad + \sum_{t=t_0}^{t_0+T} \sum_{m=1}^{M} \Bigg\{\left[P_m^{k+1}(t) - P_m^k(t)\right]^2 \\
&\qquad - \sum_{n\in\mathcal{N}_m(t_0)} \gamma_n\left(x_n^{k+1}(t) - x_n^k(t)\right)\Bigg\} \\
&\quad + \sum_{t=t_0}^{t_0+T} \sum_{m=1}^{M} \lambda_{m,t}\left(P_m^{k+1}(t) - P_m^k(t)\right) \\
&\leq \sum_{t=t_0}^{t_0+T} \Bigg\{\sum_{n\in\mathcal{N}_m(t_0)} \gamma_n\left(x_n^{k+1}(t) - x_n^k(t)\right) \\
&\qquad - 2\beta_{n,t}\left(x_n^{k+1}(t) - x_n^k(t)\right)^2 \\
&\qquad + \sum_{t=t_0}^{t_0+T} \sum_{m=1}^{M} \left[P_m^{k+1}(t) - P_m^k(t)\right]^2 \\
&\qquad - \sum_{n\in\mathcal{N}_m(t_0)} \gamma_n\left(x_n^{k+1}(t) - x_n^k(t)\right)\Bigg\} \\
&\leq -\sum_{t=t_0}^{t_0+T} \sum_{m=1}^{M} \sum_{n\in\mathcal{N}_m(t_0)} \left(2\beta_{n,t} - N_m(t_0)\left(x_n^k(t) - x_n^{k+1}(t)\right)^2\right.
\end{aligned} \tag{30}$$

where the first inequality is attained based on (28), and the second inequality is derived based on Jessen's inequality.

From (30), we note that if we have $2\beta_{n,t} \geq N_m(t_0)+1$ ($\forall n \in \mathcal{N}_m(t_0)$, i.e., $\beta_{n,t} \geq (N_m(t_0)+1)/2$ ($\forall n \in \mathcal{N}_m(t_0)$), we can derive that

$$\begin{aligned}&\mathtt{L}(t_0; \boldsymbol{x}^{k+1}, \boldsymbol{\lambda}^p) - \mathtt{L}(t_0; \boldsymbol{x}^k, \boldsymbol{\lambda}^p)\\ &\qquad \leq -\sum_{t=t_0}^{t_0+T}\sum_{m=1}^{M}\sum_{n\in\mathcal{N}_m(t_0)}\left(x_n^k(t) - x_n^{k+1}(t)\right)^2 \leq 0. \quad (31)\end{aligned}$$

This implies that the global Lagrangian objective function over each planning horizon will be nonincreasing with the number of iterations. Moreover, it is straightforward that $\mathtt{L}(t_0; \boldsymbol{x}^{k+1}, \boldsymbol{\lambda}^p) = \mathtt{L}(t_0; \boldsymbol{x}^k, \boldsymbol{\lambda}^p)$ can be reached if and only if $\boldsymbol{x}_n^k = \boldsymbol{x}_n^{k+1}$, $\forall n \in \mathcal{N}_m(t_0), m = 1, 2, \ldots, M$.

Furthermore, if we encounter $\boldsymbol{x}_n^{k+1} = \boldsymbol{x}_n^k$, ($\forall n \in \mathcal{N}$) at iteration $k+1$, we can derive from (27) that

$$\sum_{t=t_0}^{t_0+T}\sum_{m=1}^{M}\left(2(P_m^k(t) - \overline{W}_m(t)) + \lambda_{m,t}^p\right)\left(P_m(t) - P_m^k(t)\right) \geq 0. \quad (32)$$

It is easily noted that (32) is the first-order optimality condition of the convex problem (13) with the optimal solution $\boldsymbol{P}^* = \boldsymbol{P}^k = [P_m^k(t)]$. This implies that the EBDC algorithm can converge to the optimal solution of the centralized Lagrangian optimization problem (13) over each planning horizon $[t_0, t_0 + T]$.

REFERENCES

[1] International Energy Agency. (2016). *Global EV Outlook 2016*. [Online]. Available: https://www.iea.org/publications/freepublications/publication/Global_EV_Outlook_2016.pdf

[2] J. Hu, S. You, M. Lind, and J. Ostergaard, "Coordinated charging of electric vehicles for congestion prevention in the distribution grid," *IEEE Trans. Smart Grid*, vol. 5, no. 2, pp. 703–711, Mar. 2014.

[3] A. Ipakchi and F. Albuyeh, "Grid of the future," *IEEE Power Energy Mag.*, vol. 7, no. 2, pp. 52–62, Mar./Apr. 2009.

[4] S. M. Elnozahy and M. A. M. Salama, "A comprehensive study of the impacts of PHEVs on residential distribution networks," *IEEE Trans. Sustain. Energy*, vol. 5, no. 1, pp. 332–342, Jan. 2014.

[5] A. Dutton, J. Halliday, and M. J. Blanch, "The feasibility of building-mounted/integrated wind turbines (BUWTs): Achieving their potential for carbon emission reductions," Energy Res. Unit, Sci. Technol. Facilities Council Rutherford Appleton Lab., Oxfordshire, U.K., Tech. Rep. 2002-7-28-1-6, 2005, pp. 77–83.

[6] T. F. Ishugah, Y. Li, R. Z. Wang, and J. K. Kiplagat, "Advances in wind energy resource exploitation in urban environment: A review," *Renew. Sustain. Energy Rev.*, vol. 37, pp. 613–626, Sep. 2014.

[7] J. Gabel, M. Carver, and M. Gerometta. (2016). *CTBUH Year in Review: Tall Trends of 2015, and Forecasts for 2016*. [Online]. Available: http://www.skyscrapercenter.com/research/CTBUH_ResearchReport_2015YearInReview.pdf

[8] N. Mithraratne, "Roof-top wind turbines for microgeneration in urban houses in New Zealand," *Energy Buildings*, vol. 41, no. 10, pp. 1013–1018, 2009.

[9] A. Gagliano, F. Nocera, F. Patania, and A. Capizzi, "Assessment of micro-wind turbines performance in the urban environments: An aided methodology through geographical information systems," *Int. J. Energy Environ. Eng.*, vol. 4, no. 1, p. 43, 2013.

[10] W. Kempton and S. E. Letendre, "Electric vehicles as a new power source for electric utilities," *Transp. Res. D, Transp. Environ.*, vol. 2, no. 3, pp. 157–175, 1997.

[11] J. Tang, A. Brouste, and K. L. Tsui, "Some improvements of wind speed Markov chain modeling," *Renew. Energy*, vol. 81, pp. 52–56, Sep. 2015.

[12] A. Kusiak and W. Li, "Short-term prediction of wind power with a clustering approach," *Renew. Energy*, vol. 35, no. 10, pp. 2362–2369, 2010.

[13] E. Gallestey, A. Stothert, M. Antoine, and S. Morton, "Model predictive control and the optimization of power plant load while considering lifetime consumption," *IEEE Trans. Power Syst.*, vol. 17, no. 1, pp. 186–191, Feb. 2002.

[14] Y. Cao *et al.*, "An optimized EV charging model considering TOU price and SOC curve," *IEEE Trans. Smart Grid*, vol. 3, no. 1, pp. 388–393, Mar. 2012.

[15] Z. Ma, D. S. Callaway, and I. A. Hiskens, "Decentralized charging control of large populations of plug-in electric vehicles," *IEEE Trans. Control Syst. Technol.*, vol. 21, no. 1, pp. 67–78, Jan. 2013.

[16] S. Han, S. Han, and K. Sezaki, "Development of an optimal vehicle-to-grid aggregator for frequency regulation," *IEEE Trans. Smart Grid*, vol. 1, no. 1, pp. 65–72, Jun. 2010.

[17] T. Zhang, W. Chen, Z. Han, and Z. Cao, "Charging scheduling of electric vehicles with local renewable energy under uncertain electric vehicle arrival and grid power price," *IEEE Trans. Veh. Technol.*, vol. 63, no. 6, pp. 2600–2612, Jul. 2014.

[18] W. Leterme, F. Ruelens, B. Claessens, and R. Belmans, "A flexible stochastic optimization method for wind power balancing with PHEVs," *IEEE Trans. Smart Grid*, vol. 5, no. 3, pp. 1238–1245, May 2014.

[19] Y. Guo, J. Xiong, S. Xu, and W. Su, "Two-stage economic operation of microgrid-like electric vehicle parking deck," *IEEE Trans. Smart Grid*, vol. 7, no. 3, pp. 1703–1712, May 2016.

[20] Q. Huang, Q. S. Jia, Z. Qiu, X. Guan, and G. Deconinck, "Matching EV charging load with uncertain wind: A simulation-based policy improvement approach," *IEEE Trans. Smart Grid*, vol. 6, no. 3, pp. 1425–1433, May 2015.

[21] Q. Huang, Q.-S. Jia, and X. Guan, "A multi-timescale and bilevel coordination approach for matching uncertain wind supply with EV charging demand," *IEEE Trans. Autom. Sci. Eng.*, vol. 14, no. 2, pp. 694–704, Apr. 2016.

[22] Q. Huang, Q.-S. Jia, and X. Guan, "Robust scheduling of EV charging load with uncertain wind power integration," *IEEE Trans. Smart Grid*, vol. 9, no. 2, pp. 1043–1054, Mar. 2018.

[23] Y. Yang, Q.-S. Jia, G. Deconinck, X. Guan, Z. Qiu, and Z. Hu, "Distributed coordination of EV charging with renewable energy in a microgrid of building," *IEEE Trans. Smart Grid*, to be published, doi: 10.1109/TSG.2017.2707103.

[24] Q.-S. Jia, Y. Yang, L. Xia, and X. Guan, "A tutorial on event-based optimization with application in energy Internet," (in Chinese), *Control Theory Appl.*, vol. 35, no. 1, pp. 32–40, Jan. 2018.

[25] P. Kou, D. Liang, L. Gao, and F. Gao, "Stochastic coordination of plug-in electric vehicles and wind turbines in microgrid: A model predictive control approach," *IEEE Trans. Smart Grid*, vol. 7, no. 3, pp. 1537–1551, May 2016.

[26] E. M. P. Walraven and M. T. J. Spaan, "Planning under uncertainty for aggregated electric vehicle charging with renewable energy supply," in *Proc. 22nd Eur. Conf. Artif. Intell.*, 2016, pp. 904–912.

[27] J. C. Mukherjee and A. Gupta, "Distributed charge scheduling of plug-in electric vehicles using inter-aggregator collaboration," *IEEE Trans. Smart Grid*, vol. 8, no. 1, pp. 331–341, Jan. 2017.

[28] R. Jin, B. Wang, P. Zhang, and P. B. Luh, "Decentralised online charging scheduling for large populations of electric vehicles: A cyber-physical system approach," *Int. J. Parallel, Emergent Distrib. Syst.*, vol. 28, no. 1, pp. 29–45, 2013.

[29] J. C. Mukherjee and A. Gupta, "A review of charge scheduling of electric vehicles in smart grid," *IEEE Syst. J.*, vol. 9, no. 4, pp. 1541–1553, Dec. 2015.

[30] T. Wu, Q. Yang, Z. Bao, and W. Yan, "Coordinated energy dispatching in microgrid with wind power generation and plug-in electric vehicles," *IEEE Trans. Smart Grid*, vol. 4, no. 3, pp. 1453–1463, Sep. 2013.

[31] S. Bahrami and M. Parniani, "Game theoretic based charging strategy for plug-in hybrid electric vehicles," *IEEE Trans. Smart Grid*, vol. 5, no. 5, pp. 2368–2375, Sep. 2014.

[32] S. Bae and A. Kwasinski, "Spatial and temporal model of electric vehicle charging demand," *IEEE Trans. Smart Grid*, vol. 3, no. 1, pp. 394–403, Mar. 2012.

[33] I. Morro-Mello, A. Padilha-Feltrin, and J. D. Melo, "Spatial-temporal model to estimate the load curves of charging stations for electric vehicles," in *Proc. IEEE PES Innov. Smart Grid Technol. Conf.-Latin Amer. (ISGT Latin America)*, Sep. 2017, pp. 1–6.

[34] X. Guan, Z. Xu, and Q.-S. Jia, "Energy-efficient buildings facilitated by microgrid," *IEEE Trans. Smart Grid*, vol. 1, no. 3, pp. 243–252, Dec. 2010.

[35] M. Kolhe, T. C. Lin, and J. Maunuksela, "GA-ANN for short-term wind energy prediction," in *Proc. Asia–Pacific Power Energy Eng. Conf. (APPEEC)*, 2011, pp. 1–6.

[36] M. Milligan, M. Schwartz, and Y. Wan, "Statistical wind power forecasting models: Results for U.S. wind farms," Nat. Renew. Energy Lab., Golden, CO, USA, Tech. Rep. NREL/CP-500-33956, 2003.

[37] J. Wang, M. Shahidehpour, and Z. Li, "Security-constrained unit commitment with volatile wind power generation," *IEEE Trans. Power Syst.*, vol. 23, no. 3, pp. 1319–1327, Aug. 2008.

[38] D. P. Bertsekas, *Nonlinear Programming*. Belmont, MA, USA: Athena Scientific, 1999.

[39] S. Shahidinejad, E. Bibeau, and S. Filizadeh, "Statistical development of a duty cycle for plug-in vehicles in a North American urban setting using fleet information," *IEEE Trans. Veh. Technol.*, vol. 59, no. 8, pp. 3710–3719, Oct. 2010.

[40] T.-K. Lee, Z. Bareket, T. Gordon, and Z. S. Filipi, "Stochastic modeling for studies of real-world PHEV usage: Driving schedule and daily temporal distributions," *IEEE Trans. Veh. Technol.*, vol. 61, no. 4, pp. 1493–1502, May 2012.

[41] A. Santos, N. McGuckin, H. Y. Nakamoto, D. Gray, and S. Liss, "Summary of travel trends: 2009 National Household Travel Survey," U.S. Dept. Transp., Federal Highway Admin., Washington, DC, USA, Tech. Rep. FHWA-PL-ll-022, 2011.

[42] J. Liu, "Electric vehicle charging infrastructure assignment and power grid impacts assessment in Beijing," *Energy Policy*, vol. 51, pp. 544–557, Dec. 2012.

[43] H. Liu, C. He, J. Lents, N. Davis, M. Osses, and N. Nikkila, "Beijing vehicle activity study," Int. Sustain. Syst. Res. Center, La Habra, CA, USA, Final Rep., 2005.

[44] S. L. Walker, "Building mounted wind turbines and their suitability for the urban scale—A review of methods of estimating urban wind resource," *Energy Buildings*, vol. 43, no. 8, pp. 1852–1862, 2011.

[45] International Energy Agency. (2016). *Forecast and Reports of Windfinder*. [Online]. Available: https://www.windfinder.com/windstatistics/beijingcapitalairport

[46] Y. Zhang and Q.-S. Jia, "Optimal storage battery scheduling for energy-efficient buildings in a microgrid," in *Proc. 27th Chin. Control Decis. Conf. (CCDC)*, May 2015, pp. 5540–5545.

[47] Y. Zhang and Q.-S. Jia, "A simulation based policy improvement method for joint-operation of building microgrids with distributed solar power and battery," *IEEE Trans. Smart Grid*, to be published.

[48] Y. Zhang and Q.-S. Jia, "Operational optimization for microgrid of buildings with distributed solar power and battery," *Asian J. Control*, vol. 19, no. 3, pp. 996–1008, 2017.

[49] Z. Xu, Q.-S. Jia, and X. Guan, "Supply demand coordination for building energy saving: Explore the soft comfort," *IEEE Trans. Autom. Sci. Eng.*, vol. 12, no. 2, pp. 656–665, Apr. 2015.

[50] B. Sun, P. B. Luh, Q. S. Jia, and B. Yan, "Event-based optimization within the Lagrangian relaxation framework for energy savings in HVAC systems," *IEEE Trans. Autom. Sci. Eng.*, vol. 12, no. 4, pp. 1396–1406, Oct. 2015.

[51] Q. S. Jia, H. Wang, Y. Lei, Q. Zhao, and X. Guan, "A decentralized stay-time based occupant distribution estimation method for buildings," *IEEE Trans. Autom. Sci. Eng.*, vol. 12, no. 4, pp. 1482–1491, Oct. 2015.

[52] Z. Wu, Q.-S. Jia, and X. Guan, "Optimal control of multiroom HVAC system: An event-based approach," *IEEE Trans. Control Syst. Technol.*, vol. 24, no. 2, pp. 662–669, Mar. 2015.

[53] Q.-S. Jia, J. Wu, Z. Wu, and X. Guan, "Event-based HVAC control: A complexity-based approach," *IEEE Trans. Autom. Sci. Eng.*, to be published.

[54] J. Wang, Q.-S. Jia, G. Huang, and Y. Sun, "Event-driven optimal control of central air-conditioning systems: Event-space establishment," *Sci. Technol. Built Environ.*, to be published, doi: 10.1080/23744731.2018.1457410.

[55] L. Xia, Q.-S. Jia, and X.-R. Cao, "A tutorial on event-based optimization—A new optimization framework," *Discrete Event Dyn. Syst., Theory Appl.*, vol. 24, no. 2, pp. 103–132, 2014.

Yu Yang (S'14) received the B.E. degree from the School of Automation, Huazhong University of Science and Technology, Wuhan, Hubei, China, in 2013. She is currently pursuing the Ph.D. degree with the Center for Intelligent and Networked Systems, Department of Automation, Tsinghua University, Beijing, China.

Her current research interests include energy dispatching in smart grids, electric vehicle charging optimization, and decentralized optimization for large-scale dynamic systems.

Qing-Shan Jia (S'02–M'06–SM'11) received the B.E. and Ph.D. degrees in automation and control science and engineering from Tsinghua University, Beijing, China, in 2002 and 2006, respectively.

He was a Visiting Scholar with Harvard University, Cambridge, MA, USA, The Hong Kong University of Science and Technology, Hong Kong, and the Massachusetts Institute of Technology, Cambridge, MA, USA, in 2006, 2010, and 2013, respectively. He is currently an Associate Professor with the Center for Intelligent and Networked Systems, Department of Automation, Beijing National Research Center for Information Science and Technology, Tsinghua University. His current research interest is optimization for cyber-physical energy systems.

Xiaohong Guan (M'93–SM'95–F'07) received the B.S. and M.S. degrees in control engineering from Tsinghua University, Beijing, China, in 1982 and 1985, respectively, and the Ph.D. degree in electrical engineering from the University of Connecticut, Storrs, CT, USA, in 1993.

He was a Senior Consulting Engineer with PG&E, San Francisco, CA, USA, from 1993 to 1995. He visited the Division of Engineering and Applied Science, Harvard University, Cambridge, MA, USA, from 1999 to 2000. Since 1995, he has been with the Systems Engineering Institute, Xi'an Jiaotong University, Xi'an, China, and was appointed as a Cheung Kong Professor of Systems Engineering in 1999 and the Dean of the School of Electronic and Information Engineering in 2008. Since 2001, he has also been with the Center for Intelligent and Networked Systems, Tsinghua University, where he served as the Head of the Department of Automation from 2003 to 2008. He is an academician of the Chinese Academy of Sciences, Beijing. His research interests include optimization of electrical power and energy systems, markets, and cyber-physical systems such as smart grids and sensor networks.

Dr. Guan is serving as an Editor for the IEEE TRANSACTIONS ON SMART GRID.

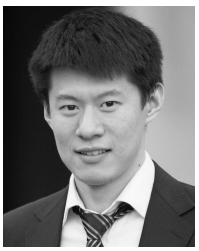

Xuan Zhang received the B.Eng. degree in automation from Tsinghua University, Beijing, China, in 2011, and the Ph.D. degree in control and electrical engineering from the University of Oxford, Oxford, U.K., in 2015.

From 2015 to 2018, he was a Post-Doctoral Fellow with the School of Engineering and Applied Sciences and the Harvard Center for Green Buildings and Cities, Harvard University, Cambridge, MA, USA. Since 2018, he has been with the Tsinghua–Berkeley Shenzhen Institute, Shenzhen, China, where he is currently an Assistant Professor with the Smart Grid and Renewable Energy Laboratory. His current research interests include the control and optimization for cyber-physical systems, such as smart grids, smart buildings, and Energy Internet, control system structure (re)design, and learning-based control.

Zhifeng Qiu (S'07–M'13) received the M.S. degree in control engineering from Central South University, Changsha, China, and the Ph.D. degree in electrical engineering from KU Leuven, Leuven, Belgium, in 2004 and 2013, respectively.

She is currently with Central South University. Her research interests include techno-economic problems in power systems and game-theoretic-based analysis of power market and integration of renewable energy into smart building.

Geert Deconinck (S'88–M'96–SM'00) received the M.Sc. degree in electrical engineering and the Ph.D. degree in applied sciences from the Katholieke Universiteit Leuven (KU Leuven), Leuven, Belgium, in 1991 and 1996, respectively.

He is a Full Professor with KU Leuven. His research focuses on robust-distributed coordination and control, specifically in the context of smart electric distribution networks. In this field, he has authored and co-authored over 440 publications in international journals and conference proceedings. He is the head of the Electrical Energy and Computing Architectures Research Group, Department of Electrical Engineering and is a scientific leader for the research domain algorithms, modeling, and optimization with EnergyVille, Leuven.

Dr. Deconinck is a fellow of the Institute of Engineering and Technology and a member of Cigr, KBVE, and ie-net.